

Invited Review

Polyfunctional Two- (2D) and Three- (3D) Dimensional Oxalate Bridged Bimetallic Magnets

René Clément¹, Silvio Decurtins², Michel Gruselle³, and Cyrille Train^{3,*}

¹ Laboratoire de Chimie Inorganique, UMR-CNRS, 8613, Université Paris Sud, F-91405 Orsay Cedex, France

² Departement für Chemie und Biochemie, Universität Bern, CH-3012 Bern, Switzerland

³ Laboratoire de Chimie Inorganique et Matériaux Moléculaires, CIM² UMR-CNRS, 7071, Université Pierre et Marie Curie, F-75252 Paris Cedex 05, France

Received April 11, 2002; accepted May 27, 2002

Published online January 8, 2003 © Springer-Verlag 2003

Summary. We report major results concerning polyfunctional two- (2D) and three- (3D) dimensional oxalate bridged bimetallic magnets. As a consequence of their specific organisation they are composed of an anionic sub-lattice and a cationic counter-part. These bimetallic polymers can accommodate various counter-cations possessing specific physical properties in addition to the magnetic ones resulting from the interactions between the metallic ions in the anionic sub-lattice. Thus, molecular magnets possessing paramagnetic, conductive and optical properties are presented in this review.

Keywords. Oxalate; Molecular magnets; NLO; Photochromism; Cotton effect; Fluorescence.

1. Introduction

1.1 Why polyfunctional materials?

The need for new materials that have more diversified and more sophisticated properties is continuously increasing [1]. Opportunities offered by the flexibility of inorganic chemistry led to a blossoming of new research fields in inorganic molecular materials [2]. One of the goals is to obtain materials that possess not only one expected property (mechanical, optical, magnetic, electric . . .) but also

* Corresponding author. E-mail: train@cct.jussieu.fr

combine two or more of them in polyfunctional systems. For example, in the field of molecular magnetism [3], superconducting paramagnets [4], photomagnetic ferrimagnets [5] and room temperature magnets [6] were reported.

1.2 Polyfunctional molecular magnets

Polyfunctional molecule based magnets represent an important class of polyfunctional materials. Their magnetic properties (ferro-, ferri-, anti-ferro) depend on the nature of the interacting metal ions [3a]. These magnetic properties can be modulated by the nature of the bridging ligand and also by the whole structure and environment created by the supramolecular arrangement of the building blocks. Additional physical properties can be introduced by different ways: (i) the ligand can be the centre of this phenomenon when bearing a specific property, for example optic in the case of an optically active ligand, magnetic when the ligand is a free radical; (ii) one of the building blocks can possess a specific property like chirality or fluorescence activity; (iii) when the materials comprise two sub-lattices (hybrid materials), one of them can bring out the magnetic properties while the other one brings a different property.

1.3 Oxalate based magnets

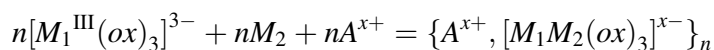
In literature, many oxalate based magnets are described. They can occur as poly-metallic discrete entities – named 0D – in which transition metal ions interact through the oxalate ligand [7]. These systems are of importance to understand the nature of the orbital exchange at the molecular level. Chains (1D) [8], layered (2D) and three-dimensional structures (3D) [9] are also known. In these structures the oxalate ligand bridging the metal ions can be replaced by a dithiooxalate ligand [10], a change that leads to modifications in both the exchange interaction J values (magnetic effect) and the size of the basic structure of the polymer (structural effect). In other cases, 2,2'-bipyridine [11], 4,4'-bipyridine [12], or 2,2'-bipyrimidine [13] were used together with oxalate ligand to synthesise compounds with mixed bridging ligands.

In the scope of this review, we restrict ourselves to the major works published on polyfunctional tris(oxalato)metalate based magnets.

2. Tris(oxalato)metalate Based Magnets

2.1 2D and 3D structures

In the last few years *Okawa* [14], *Decurtins* [15], *Day* [16], *Coronado* [17], and *Ovanesyan* [18] have thoroughly investigated two- and three-dimensional networks (noted 2D and 3D) prepared from the combination of tris(oxalato)metalates, $[M^{\text{III}}(\text{ox})_3]^{3-}$ ($M^{\text{III}} = \text{Cr}, \text{Co}, \text{Fe}, \text{Ru}$), with other metallic precursors such as alkali cations (Li^+ , Na^+) or di-cationic transition metal ions (Mn^{2+} , Ni^{2+} , Fe^{2+} ...), according to the reaction:



These bimetallic networks of general formula $\{A^{x+}, [M_1M_2(ox)_3]^{x-}\}_n$ (noted $[M_1M_2]$) are composed of an anionic sub-lattice $\{[M_1M_2(ox)_3]^{x-}\}_n$ and a cationic counter-part $[A^{x+}]_n$. In these compounds, the charge of each sub-unit of the anionic sub-lattice is one or two according to the oxidation state of each metal centre. For instance, it is (-1) for $[M_1^{II}M_2^{III}(ox)_3]^{1-}$ and (-2) for $[M_1^I M_2^{III}(ox)_3]^{2-}$.

When two transition metal ions are connected through the oxalate ligands, exchange interaction occurs leading to a magnetic order below the *Curie* temperature T_c . The ferro-, (canted) antiferro- or ferri-magnetic properties depend on the nature of the connected metal ions.

Additionally, such tris(bidentate) complexes display a propeller-like chirality [19]. Therefore each chiral element exists as Δ or Λ enantiomeric forms [20] (noted ΔM or ΛM), as shown in Fig. 1. Furthermore, the relative configuration of the connected hexacoordinated centres (Fig. 2) determines the 2D or 3D architecture of the polymer. A hetero-chiral arrangement $[\Delta M_1-\Lambda M_2]$ or $[\Lambda M_1-\Delta M_2]$ leads to a 2D network (Fig. 2a). In this situation the anionic sub-lattice displays a honeycomb structure while the cationic moiety, which is in general a tetra-alkyl ammonium (NR_4^+) [21, 22] or phosphonium (PR_4^+) [15, 23, 24] ion, is located between the anionic layers. On the other hand, a homo-chiral arrangement $[\Delta M_1-\Delta M_2]$ or $[\Lambda M_1-\Lambda M_2]$ leads to a helical organisation of the connected metallic ions (Fig. 2b). Therefore a three dimensional structure is obtained giving a 3-connected decagon anionic network with the associated cationic counter-part fitting in the vacancies (Fig. 3) [25, 26].

To build such 2D and 3D networks in an optically active form, two geometrical elements must be controlled:

- The absolute Δ or Λ configuration of each hexacoordinated metal centre.
- The relative configuration of the adjacent metal centres.

The nature of the template cation appears as a determining factor to orient the reaction towards 2D or 3D structures. Three elements have to be taken in consideration: the charge, the size and the symmetry of the cation.

The *charge* of the template cation has to be equal to the charge of the anionic sub-unit $[M_1M_2(ox)_3]^{x-}$ ($x=1$ or 2). Therefore the template cations are

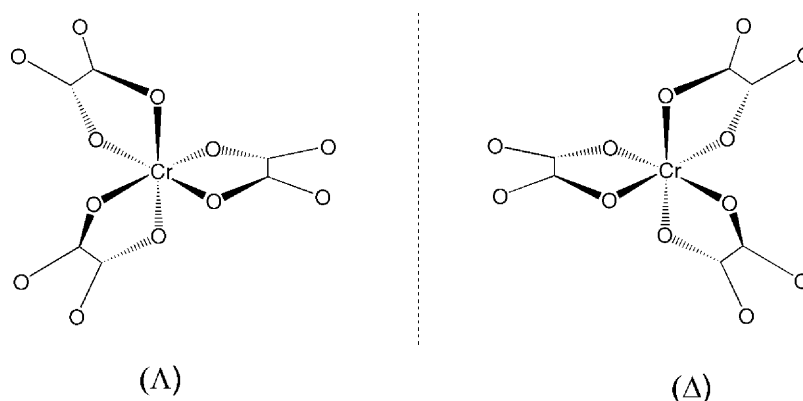


Fig. 1. Δ and Λ enantiomeric forms of $[Cr(ox)_3]^{3-}$

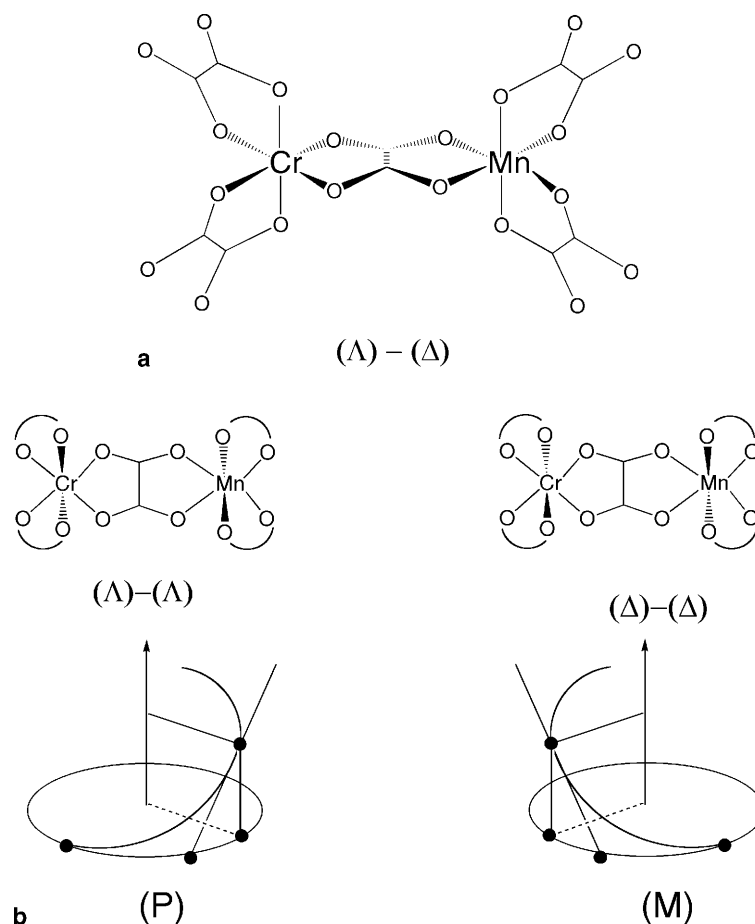


Fig. 2. Relative hetero- (a) or homo-chiral (b) arrangement of oxalate bridged centres

mono- or di-cations (tetra-alkyl Ammonium or Phosphonium, $[\text{Ni}(\text{phen})_3]^{2+}$, $[\text{Ru}(\text{bpy})_3]^{2+}$, ... with *phen* = phenantroline, *bpy* = bipyridine). When the charge of the anionic sub-unit is (-1) , mono-cations belonging to hexacoordinated metal complexes were also used, namely: $[\text{Ru}(\text{bpy})_2(\text{ppy})]^+$, $[\text{Ru}(\text{bpy})_2(\text{quo})]^+$ with *ppy* = (2-phenylpyridine - H^+), *quo* = 8-Hydroxyquinoleate [27]. In certain cases, a di-cation in tandem with a mono-anion can be used in place of a mono-cation: for example $[\text{Ru}(\text{bpy})_3\text{ClO}_4]^+$ [17, 27].

The size of the template cation is of primary importance, allowing or not the formation of the anionic framework. In 2D networks, along the series of highly symmetrical tetra-alkyl ammonium salts it was shown that the anionic auto-assembling process is possible from $R = n$ -propyl to n -pentyl. In the case of the $[\text{Fe}^{\text{II}}\text{Fe}^{\text{III}}]$ or $[\text{Mn}^{\text{II}}\text{Fe}^{\text{III}}]$ compounds, the inter-layer distances were systematically investigated by Day [24b], varying from 8.2 to 10.23 Å and 8.18 to 10.15 Å, respectively. However, in the case of cations having a lower symmetry, it was found that cations of various sizes could intercalate into the anionic framework. This is the case for $[(\text{C}_6\text{H}_5)_3\text{PNP}(\text{C}_6\text{H}_5)_3]^+$ (14.43 Å) [24a] and for a series of ferrocenic ammonium salts $[\text{C}_5\text{H}_5\text{FeC}_5\text{H}_4\text{CH}_2\text{NR}_3]^+$ with $R = \text{Et, Pr, But}$ (10.0 Å) [28]. Symmetrical

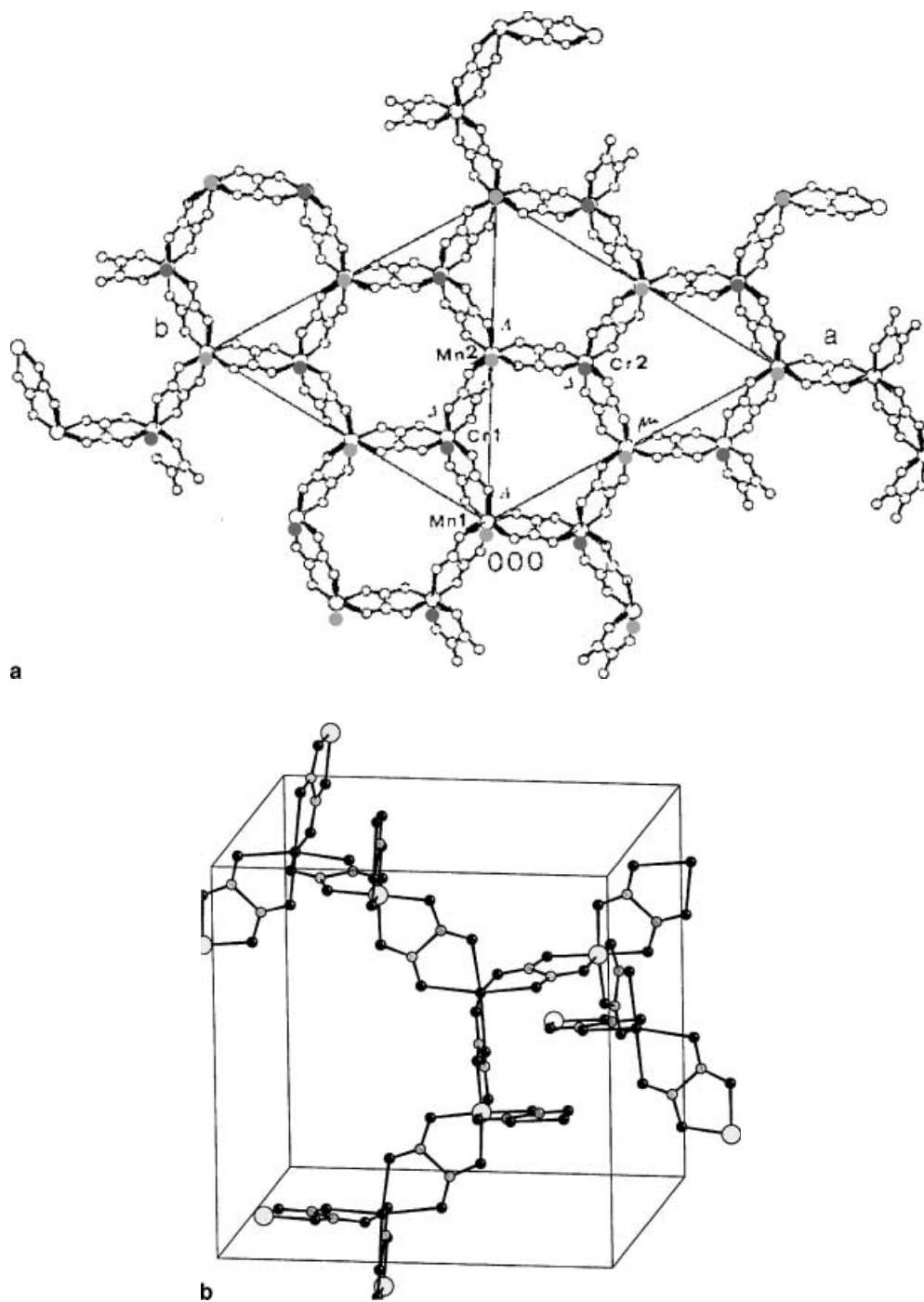


Fig. 3. (a) 2D honeycomb structure (adapted from Ref. [25b]); (b) 3D 3-connected 10-gon anionic network (adapted from Ref. [37])

phosphonium or arsenium cations [24a], are also able to template the formation of 2D anionic framework. Other cations were used as template namely stilbazolium [29], ferricinium and cobalticinium [30]. In contrast, for 3D networks the cavities

in the anionic network are such that the number of cations able to play a template role is limited: $[\text{Ni}(\text{phen})_3]^{2+}$, $[\text{Ru}(\text{bpy})_3]^{2+}$ and $[\text{Ru}(\text{bpy})_2(\text{ppy})]^+$.

The symmetry of the template cation plays an important role to orient the reaction towards 2D or 3D networks. Chiral or achiral tetra-alkyl ammonium, phosphonium, stilbazolium, ferricinium as well as ferrocenic ammonium cations lead to 2D structures. In contrast, chiral hexacoordinated metal complexes belonging to D_3 or quasi- D_3 symmetry lead to 3D networks.

2.2 Magnetic properties

Most of the magnetic properties of tris(oxalato)metalate based networks have been established on two dimensional compounds starting either from $[\text{Cr}(\text{ox})_3]^{3-}$ [14], $[\text{Fe}(\text{ox})_3]^{3-}$ [24] or $[\text{Ru}(\text{ox})_3]^{3-}$ [22].

In the former case, the exchange coupling in $\{\text{A}[\text{M}^{\text{II}}\text{Cr}^{\text{III}}(\text{ox})_3]\}_n$ is ferromagnetic (F) leading to ferromagnets with Curie temperatures (T_c) ranging from 6 ($M^{\text{II}} = \text{Mn}$) to 18 K ($M^{\text{II}} = \text{Ni}$). Starting from iron (III), the exchange coupling is antiferromagnetic (AF) leading to canted antiferromagnets ($M^{\text{II}} = \text{Mn} - T_c = 27$ K) or ferrimagnets ($M^{\text{II}} = \text{Fe} - T_c = 33\text{--}48$ K). In some $[\text{Fe}^{\text{II}}\text{Fe}^{\text{III}}]$ compounds, Day *et al.* have observed negative magnetisation below the so-called compensation temperature T_{comp} over a wide temperature range [24]. With the ruthenium (III) precursor [22], the exchange coupling in the network is AF for $M^{\text{II}} = \text{Fe}$, Cu and F for $M^{\text{II}} = \text{Mn}$. An ordered phase is observed only for $M^{\text{II}} = \text{Fe}$ ($T_c = 13$ K).

The sign and the magnitude of the exchange coupling J in these networks have been compared with those measured on 0D tetra-metallic complexes [7b, 31] and/or deduced from the orbital approach developed by Kahn [3a]. The agreement is rather good except from ruthenium (III) based magnets. This disagreement is attributed to the slight increase in the spin-orbit coupling when going from iron (III) to ruthenium (III) [22].

The existence of a long-range magnetic order in 2D compounds raises the question of the nature of the exchange coupling in these compounds. Do we have an Ising, a XY or a Heisenberg system, e.g. does the exchange coupling present some kind of anisotropy? The neutron measurement performed on $[\text{Mn}^{\text{II}}\text{Cr}^{\text{III}}]$, using NBu_4^+ as counter-cation, concludes that this system is Ising-type with an easy-axis perpendicular to the (a, b) planes [32]. Mössbauer studies on $[\text{M}^{\text{II}}\text{Fe}^{\text{III}}]$ with $M^{\text{II}} = \text{Mn}$, Fe assesses that most of these networks are XY-planar magnets [18]. In particular, for $\{(\text{NBu}_4)[\text{Mn}^{\text{II}}\text{Fe}^{\text{III}}]\}$ with 3-fold site symmetry, the unusual magnetic relaxation behavior well below T_c has been attributed to a low in-plane anisotropy constant [18b]. The Mössbauer studies lead to the same conclusion for $[\text{Fe}^{\text{II}}\text{Cr}^{\text{III}}]$ polymers [23] while the internal magnetic field changes gradually from perpendicular to parallel (to the planes) when x decreases in $\{(\text{NBu}_4)[\text{Fe}^{\text{II}}_x\text{Mn}^{\text{II}}_{1-x}\text{Cr}^{\text{III}}(\text{ox})_3]\}_n$ [33].

Exploiting the versatility of the 2D networks towards the choice of the counter cation A^+ , a great variety of cations has been introduced in these compounds leading to important variations of the interplanar distances [21, 23–24]. The value of T_c is rather sensitive to such substitution. Nevertheless, no clear correlation appears between the variations of T_c and that of the interplanar distance. A possible interpretation to the sensitiveness of T_c upon cation substitution is the Ising vs. XY nature of the exchange coupling. In the former case, there is a low influence of

substitution upon T , as observed on the [MnCr] system, because 2D *Ising* systems are able to present a long range magnetic order. On the contrary, in the latter case, additional interaction is needed in order to observe long range magnetic order instead of *Kosterlitz-Thouless* phases [34]. Structural “details” like the interplanar distance or the relative positions of metal ions of two adjacent layers then play a crucial role on the critical temperature as observed in the case of the $[\text{Fe}^{\text{II}}\text{Fe}^{\text{III}}]$ system [24].

The antagonist nature of the J value has been exploited by *Bhattacharjee et al.* [35] and *Coronado et al.* [30]. They have studied the competition between ferro- and ferri-magnetic ordering in $\{(\text{NBu}_4)[\text{Fe}^{\text{II}}(\text{Fe}^{\text{III}}_x\text{Cr}^{\text{III}}_{1-x})(\text{ox})_3]\}_n$ [35] and $\{A[M^{\text{II}}(\text{Fe}^{\text{III}}_x\text{Cr}^{\text{III}}_{1-x})(\text{ox})_3]\}_n$ ($M^{\text{II}} = \text{Mn, Fe, Co, Ni}$; $A^+ = \text{NBu}_4^+, [\text{FeCp}^*_2]^+, [\text{CoCp}^*_2]^+$). For intermediate values of x , they have observed spin-glass behaviour in these compounds.

The study of the magnetisation *vs.* field in the ordered phase revealed important variations of the coercive force H_c with the counter cation. It is yet unclear whether these variations should be attributed to intrinsic effect (structural anisotropy due to the cation, effect of the paramagnetism of the cation...) or to extrinsic effect (shape anisotropy depending on the cation). The highest coercive force in those compounds is observed in $\{[\text{CoCp}^*_2][\text{Fe}^{\text{II}}(\text{Fe}^{\text{III}}_{0.52 \pm 0.05}\text{Cr}^{\text{III}}_{0.480 \pm 0.05})(\text{ox})_3]\}_n$ [30]. It reaches 1.675 T at 2 K exploiting both the effect of the cobalticinium counter cation and the glassy behaviour of the compound.

Magnetic studies on 3D compounds are not so rich. Most of the compounds are actually paramagnets [25c, 27b] or (canted) anti-ferromagnets [36, 37, 26a]. The first studies on ferromagnetic phases came out from the strategy developed by *Coronado et al.* [26b] and *Andrés et al.* [27a, b] that allowed the synthesis of $\{[M_1^{\text{II}}M_2^{\text{III}}(\text{ox})_3]_n\}^{n-}$ 3D anionic network (see above). The general trends appear to be a decrease of T_c compared to the parent 2D compounds while the identity of the $[M_1^{\text{II}}M_2^{\text{III}}(\text{ox})_3]$ pattern should lead to similar exchange coupling and hence critical temperature. This evolution can be tentatively attributed to the relative stiffness of the network imposed by the use of a template cation which prevent the oxalate bridge from adopting the geometry that maximises the J value. In such a vision, an interesting magneto-structural correlation has been made by *Andrés et al.* [27b] on $\{[\text{Ru}(\text{bpy})_3][\text{ClO}_4][\text{MnCr}(\text{ox})_3]\}_n$ and $\{[\text{Ru}(\text{bpy})_2(\text{ppy})][\text{MnCr}(\text{ox})_3]\}_n$. In the former case, the oxalate bridge is rather unsymmetrical leading to a low value of T_c . In the later case, the oxalate-bridge is symmetrical leading to a value of T_c close to the one observed in 2D $[\text{Mn}^{\text{II}}\text{Cr}^{\text{III}}]$ networks.

3. Polyfunctional Tris(oxalato)bimetallic Based Magnets

To the long-range magnetic order arising from the anionic network, it is possible to add another physical property. This property can come from (i) a proper choice of the cationic counter part, (ii) the whole structure itself, and (iii) a combination of the two previous effect.

3.1 Magnetism and magnetism

Among the counter cations introduced in these networks, some are paramagnetic species. The use of ferricinium cation leads to 2D compounds [30] which combines

a long-range magnetic order due to the anionic network with the paramagnetic properties of the cationic counterpart. The use of $[M^{\text{II}}(\text{bpy})_3]^{2+}$ ($M^{\text{II}} = \text{Ni}^{\text{II}}, \text{Fe}^{\text{II}}, \text{Co}^{\text{II}}$) and $[\text{Cr}(\text{bpy})_3]^{3+}$ sometimes associated to a monoanion (ClO_4^- or BF_4^-) leads to three dimensional networks [15b, 27b, 17] with an anionic network which is a para-, a (canted) antiferro- or a ferro-magnets. In both 2D and 3D cases, the presented studies do not show any clear interplay between the magnetic properties of the anionic network and those of the cationic counterpart.

An interesting result obtained on 3D compounds has to be mentioned here. *Sieber et al.* [38] has shown that the magnetic properties of the template cation can be modified by a proper choice of the anionic network: the $[\text{Co}^{\text{II}}(\text{bpy})_3]^{2+}$ ion shows a thermal spin transition from high spin state to low spin state when decreasing the temperature in $\{[\text{Co}(\text{bpy})_3][\text{LiCr}(\text{ox})_3]\}_n$ while it stays in the high spin state down to 2 K in $\{[\text{Co}(\text{bpy})_3][\text{NaCr}(\text{ox})_3]\}_n$. Nevertheless, this effect is linked to structural changes in the anionic network and not to the influence of the magnetic properties of this network.

3.2 Magnetism and conduction

Kurmoo et al. [4] and *Coronado et al.* [39] have synthesised compounds including BEDT-TTF (Bis(ethylenedithio)tetrathiafulvalene) cations. *Coronado et al.* has shown that conduction and long range magnetic order coexist in $\{[\text{BEDT-TTF}]_3[\text{MnCr}(\text{ox})_3]\}_n$ [39]. The two properties seems to be nearly independent though the appearance of a negative magneto-resistance below 10 K for a magnetic field applied perpendicularly to the layers may be caused by the internal field generated at low temperature by the $\{[\text{MnCr}(\text{ox})_3]\}_n^{n-}$ magnetic layers. *Kurmoo et al.* have shown in $[\text{BEDT-TTF}]_4[(\text{H}_2\text{O})\text{Fe}(\text{ox})_3]$ that it is possible for a paramagnet to present a superconducting phase at low temperature (Fig. 4) despite the long believed antagonism between magnetism and conductivity [4].

3.3 Magnetism and optics

3.3.1 Cotton and Faraday effect

In a provocative article entitled: “Can a magnetic field induce asymmetric synthesis?” *Barron* [40] predicted that, in certain conditions, asymmetric induction might take place in a magnetic field. Recently, the discovery of the magneto-chiral dichroism (MchD) in paramagnetic chiral compounds [41] has stimulated interest in molecular material possessing both *Cotton* and *Faraday* effects. These two properties can be found simultaneously in optically active molecule based magnets. It is noteworthy that chiral magnets obtained in a racemic way were described by *Gatteschi* [42], *Inoue* [43], and *Julve* [44], but the described compounds were not obtained in an optically active form resulting from the whole structure of the network. Recently *Veciana et al.* [45] have proposed the synthesis of a molecular ferromagnet starting from bis(hexafluoroacetylacetonate)manganese(II) coordinated by an optically active nitroxide radical.

3.3.1.i 2D networks Some optically active 2D networks were obtained using as starting materials Δ or Λ $[\text{Cr}(\text{ox})_3]^{3-}$ anionic bricks in the presence of Mn^{2+} and

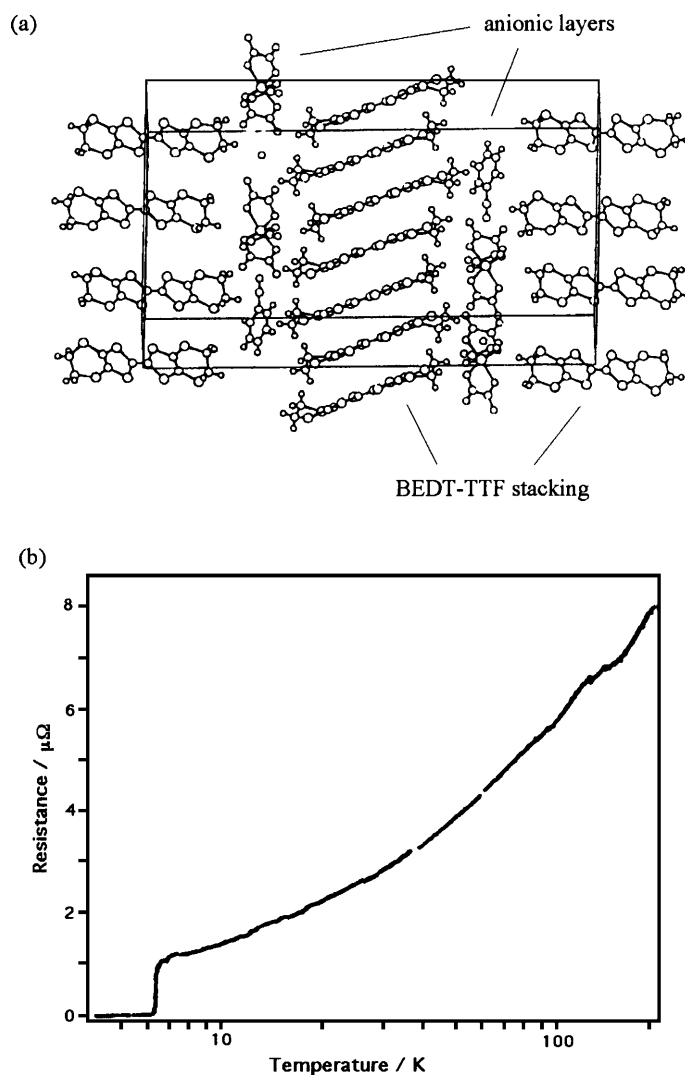


Fig. 4. Structure (a) and resistance vs. T (b) for the $\{(\text{BEDT-TTF})_4(\text{H}_2\text{O})\text{Fe}(\text{ox})_3\} \cdot \text{C}_6\text{H}_5\text{CN}\}_n$ compound (adapted from Ref. [4])

$n\text{-Bu}_4\text{N}^+$ as template cation [37]. These compounds show opposite *Cotton* effect related to the configuration Δ or Λ of the starting material. This effect is attributed to the d–d transition of chromium. Compared to the starting brick, the maxima are shifted by 20 nm. Crystallographic data recorded on powders show that the space group changes from the $R3c$ for *rac*-[MnCr] to $P6_3$ for optically active $[\Delta\text{Mn}-\Lambda\text{Cr}]$ or $[\Lambda\text{Mn}-\Delta\text{Cr}]$ compounds, indicating a significant change in the organisation of the crystal structure [46].

Others optically active 2D networks were synthesised using as starting materials Δ or Λ $[\text{Cr}(\text{ox})_3]^{3-}$ anionic bricks in the presence of Ni^{2+} or Mn^{2+} and of achiral ferrocenic ammonium salts $[\text{C}_5\text{H}_5\text{FeC}_5\text{H}_4-\text{CH}_2\text{NR}_3]^+$ with $R = n$ -ethyl to n -butyl [28, 47]. The Circular dichroism (CD) curves for $R = n$ -propyl are shown in Figure 5.

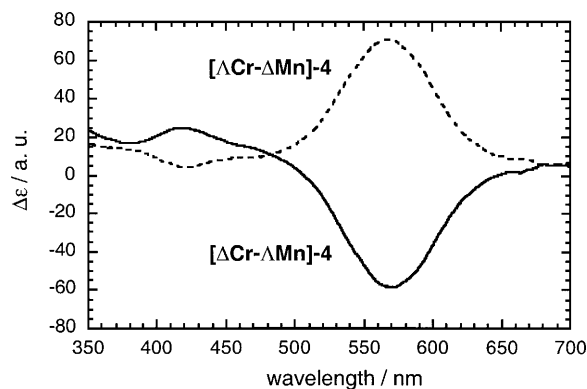


Fig. 5. Circular dichroism spectra of $[\Delta\text{Cr}-\Delta\text{Mn}]-4$ and $[\Lambda\text{Cr}-\Lambda\text{Mn}]-4$

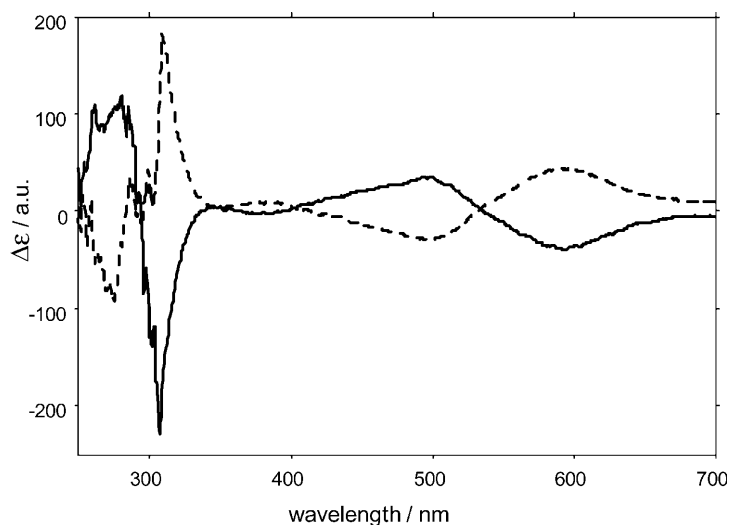


Fig. 6. Circular dichroism spectra of $M\text{-}\{[\Delta\text{Ru}(\text{bpy})_2\text{ppy}][\Delta\text{Cr}\Delta\text{Mn}(\text{ox})_3]\}_n$ (full line) and $P\text{-}\{[\Lambda\text{Ru}(\text{bpy})_2\text{ppy}][\Lambda\text{Cr}\Lambda\text{Mn}(\text{ox})_3]\}_n$ (dotted line)

3.3.1.ii 3D networks In the 3D bimetallic networks connected by oxalate ligands, chirality results from the helical auto-assembling. To build optically active materials, it is possible to use either an optically active anionic brick or an optically active cationic template. Compounds having the general formula: $\{C[M_1M_2(\text{ox})_3]\}_n$ with $C = [\text{Ru}(\text{bpy})_3]^{2+}$ [27b, 37], $[\text{Ru}(\text{bpy})_2(\text{ppy})]^+$ [27c] ($M_1 = M_2 = \text{Mn}^{2+}$; $M_1 = \text{Mn}^{2+}, \text{Ni}^{2+}, \text{Fe}^{2+}, \text{Cu}^{2+}$ and $M_2 = \text{Cr}^{3+}, \text{Co}^{3+}, \text{Fe}^{3+}$) were obtained in homochiral enantiomeric forms. CD curves for the two enantiomers (M)- $\{[\Delta\text{Ru}(\text{bpy})_2\text{ppy}][\Delta\text{Mn}\Delta\text{Cr}(\text{ox})_3]\}_n$ and (P)- $\{[\Lambda\text{Ru}(\text{bpy})_2\text{ppy}][\Lambda\text{Mn}\Lambda\text{Cr}(\text{ox})_3]\}_n$ are shown in Fig. 6.

The structures of the compounds (P)- $\{[\Lambda\text{Ru}(\text{bpy})_2\text{ppy}][\Lambda\text{Mn}\Lambda\text{Cr}(\text{ox})_3]\}_n$ and (M)- $\{[\Delta\text{Ru}(\text{bpy})_3][\text{ClO}_4][\Delta\text{Mn}\Delta\text{Cr}(\text{ox})_3]\}_n$, (Fig. 7) determined by X-ray diffraction, support the homochiral arrangement of these 3D networks.

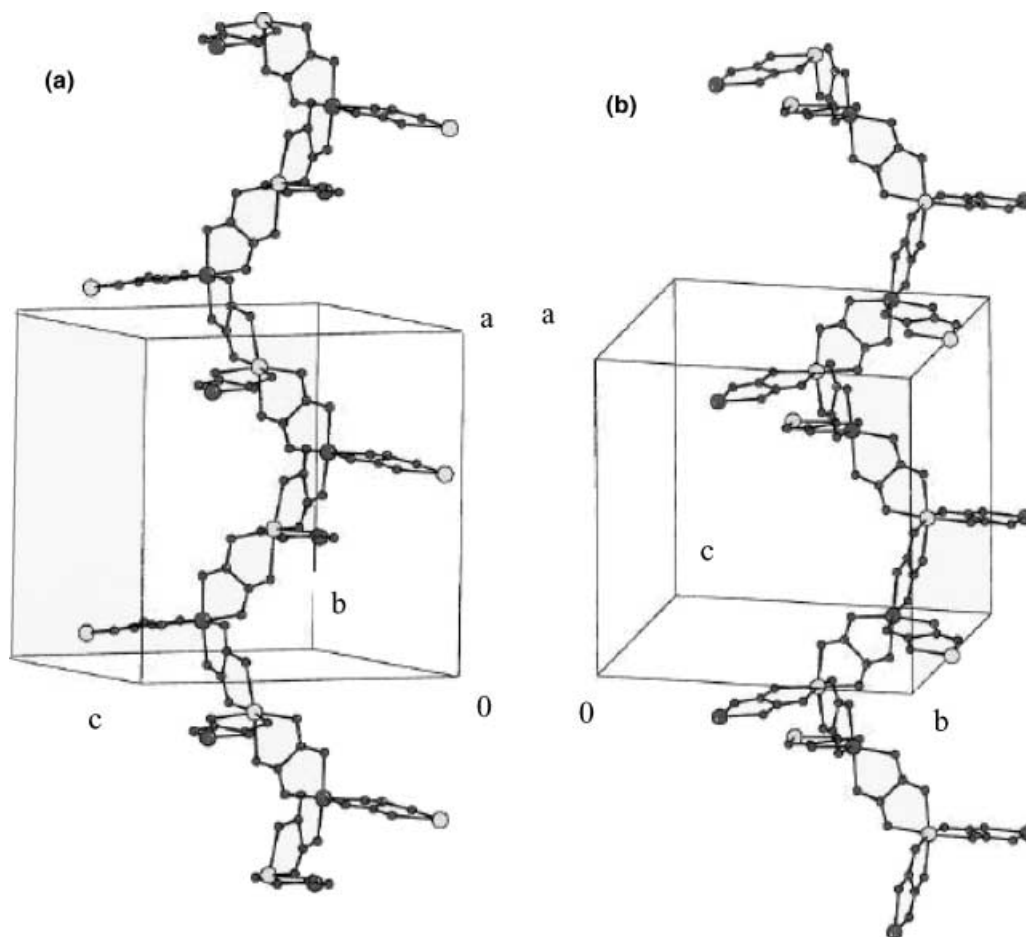


Fig. 7. Helical structures of the compounds $M\text{-}\{[\Delta Ru(bpy)_3][ClO_4][\Delta Mn\Delta Cr(ox)_3]\}_n$ (a) and $P\text{-}\{[\Delta Ru(bpy)_2ppy][\Delta Mn\Delta Cr(ox)_3]\}_n$ (b)

Together with the measurement of spectroscopic NCD (Natural circular dichroism), the magnetic measurements performed on $\{[\Delta Ru(bpy)_3][ClO_4][\Delta Mn\Delta Cr(ox)_3]\}_n$ and $\{[\Delta Ru(bpy)_2ppy][\Delta Mn\Delta Cr(ox)_3]\}_n$, establish that these compounds are the first optically active ferromagnets [27b]. $\{[\Delta Ru(bpy)_3][ClO_4][\Delta Mn\Delta Cr(ox)_3]\}_n$ has been shown to possess magnetic circular dichroism (MCD) below its *Curie* temperature. This experiment, together with the observed NCD signal, shows the capability of these compounds to exhibit an important cross-effect between NCD and MCD, the so-called magneto-chiral dichroism (MChD). It thus opens a new field of research in polyfunctional molecular materials since the measurement of such a cross effect would be an unambiguous manifestation of the possibility of interaction between two physical properties in polyfunctional molecule-based magnets [48].

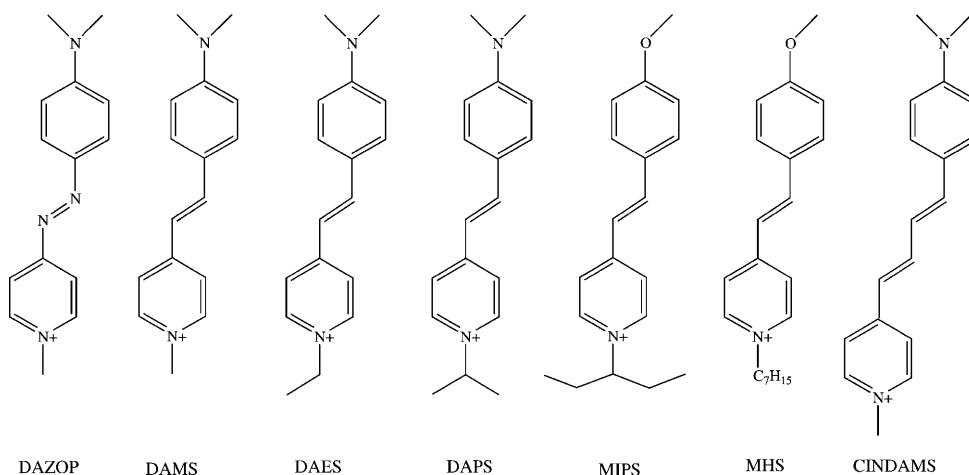
3.3.2 Quadratic non-linear optical (NLO) properties

Materials possessing large quadratic (second order) optical non linearities are of interest for their potential use in second harmonic generation (SHG), electro-optic

devices and more generally to the emerging field of photonics [49]. Up to a recent period, there were no compounds combining both a spontaneous magnetisation and second order NLO properties. The layered oxalate system provides an opportunity to incorporate hyperpolarisable cationic chromophores in between magnetic layers, which in some cases can exert a constraint strong enough to enforce a non-centrosymmetric packing of the chromophores – a pre-requisite for quadratic non linearity. This strategy has been employed to line up stilbazolium-type chromophores within the MnPS_3 layered host lattice [50]. A series of thirty five layered compounds $\{\text{A}[\text{M}^{\text{II}}\text{Cr}^{\text{III}}(\text{ox})_3\text{solvent}]\}_n$ has been synthesised with five divalent ions ($M = \text{Mn, Fe, Co, Ni, Cu}$) and the seven hyperpolarisable stilbazolium-shaped [A] chromophores shown in Scheme 1 [50, 51].

All compounds order ferromagnetically below Curie temperatures that range from 6 K to 13 K. About two third of these exhibit NLO activity, those containing DAMS or DAZOP chromophores being even particularly efficient (data in Table 1).

Despite extensive efforts, it has been only possible to grow single crystals of two (NLO-inactive) compounds ($M = \text{Mn, A} = \text{MIPS}$ and DAPS). Both of them crystallise in the centrosymmetric space group $\text{P2}_1/\text{c}$, a feature consistent with the lack of NLO effect [51]. The dipolar moments of the chromophores lying in a given organic layer are arranged in an antiparallel manner. Recently the structure of the strongly NLO active compound $\{\text{DAZOP}[\text{Mn}^{\text{II}}\text{Cr}^{\text{III}}(\text{ox})_3]\text{CH}_3\text{CN}_{0.6}\}_n$ has been solved by *Rietvelt* refining of X-ray diffraction powder data [52]. All the chromophores are



Scheme 1. The seven cationic chromophores introduced within the oxalate lattice

Table 1. Efficiency of second harmonic generation of several oxalate–chromophore hybrid compounds, expressed with respect to urea (powdered samples, incident wavelength 1.9 μm)

	DAZOP	DAMS	DAES	DAPS	MIPS	MHS	CINDAMS
[MnCr]	100	100	0	0	0	30	40
[FeCr]	19	17	5	19	4	21	10
[CoCr]	100	10	0	7	6	0	21
[NiCr]	25	25	0	0	0	0	1
[CuCr]	32	10	0	1	0	0	8

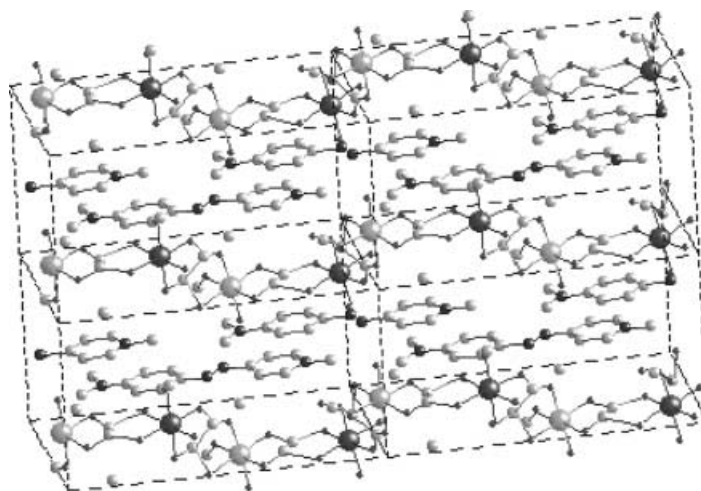


Fig. 8. The $\langle\langle$ ferroelectric $\rangle\rangle$ arrangement of the DAZOP chromophores in the $\{\text{DAZOP}[\text{MnCr}(\text{ox})_3]\}_n$ hybrid compound

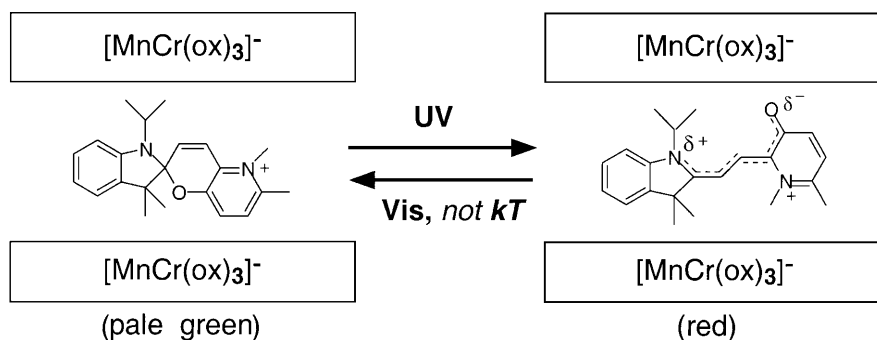
lined up in a $\langle\langle$ ferroelectric $\rangle\rangle$ way throughout the whole crystal (Fig. 8). The possible interplay between magnetic and NLO properties in this class of materials has been examined but no clear-cut effect has been evidenced so far [53].

Remarkably, the DAZOP chromophores fill in the interlayer space in an uniform way. The oxalate sheets, which are no longer puckered, come closer to each other. A search for structure-property correlation among the 35 compounds suggests that NLO activity goes along with a shorter interlayer distance. This feature in turn suggests that the gain in coulombic energy due to a closer approach of the anionic and cationic layers may counterbalance the natural tendency of the chromophores to pair up their dipolar moments.

3.3.3 Magnetism and photochromism: towards photosensitive magnetic switches

The incorporation of photosensitive organic species in between the layers of the magnetic oxalate lattice has led recently to the design of a new type of photosensitive magnetic switch. Thus, incorporation of the cationic spiropyran (SP) shown in Scheme 2, yields a hybrid compound $\{(\text{SP})[\text{Mn}^{\text{II}}\text{Cr}^{\text{III}}(\text{ox})_3]\}_n$, that exhibits an unusual set of optical and magnetic features [54]:

- (i) This compound behaves as a photochromic material, that is, the spiropyran (SP closed form) – merocyanin (MC, open form) transformation still comes about in both directions as a result of either UV irradiation (opening) or visible irradiation (closure), see Scheme 2 [55]. Remarkably, both the closed SP form and the photo-induced open MC form are found to be thermally stable, that is, there is no thermal relaxation towards the most stable of the two forms, a feature which contrasts with the usual properties of spiropyrans [56]. Most probably, this feature is due to the effect of the ionic packing forces between the anionic oxalate layers and the cationic organic layers, which increase the potential energy barrier hindering interconversion.



Scheme 2. Spiropyran–merocyanin switching process in between oxalate sheets

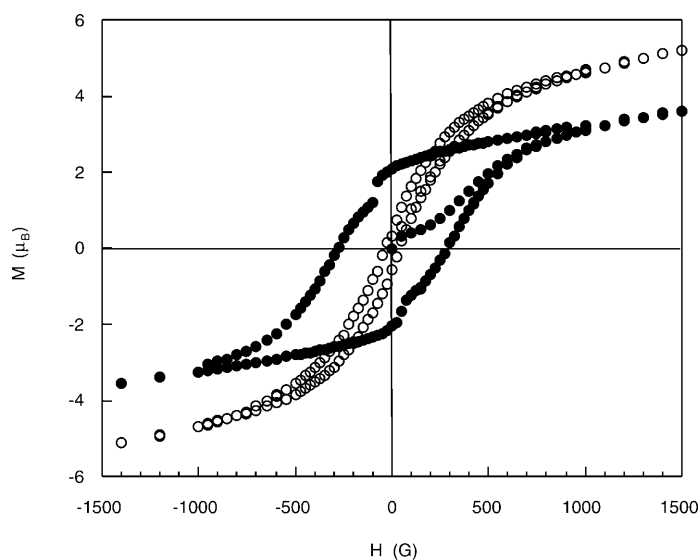


Fig. 9. Hysteresis loop at 2 K of the $\{(SP)[MnCr(ox)_3]\}_n$ compound before (white circles) and after (black circles) UV irradiation (at 365 nm)

- (ii) UV irradiation transforms the initially very soft $\{(SP)[Mn^{II}Cr^{III}(ox)_3]\}_n$ magnet into a much *harder* one, as evidenced by the change in the shape of the hysteresis loop (Fig. 9) [55].

This feature appears to be irreversible and its origin is thought to reside in the formation of structural defects and local disorder arising from the strains that must accompany the photostructural changes of the chromophores. Such defects are likely to pin the *Bloch* walls of the magnetic domains and hence decrease their mobility [57].

3.3.4 Fluorescence

In this section, a short comment on observations of excitation energy-transfer processes within the 3D supramolecular host/guest compounds will be presented. Consider that chemical variation and combination of metal ions of different valencies in the oxalate-backbone as well as in the tris-bipyridine cation offer unique

opportunities for studying a large variety of photophysical phenomena. Naturally, the sensitizer can be incorporated into the oxalate-backbone or the tris-bipyridine cation, either in low concentration as dopant, at higher concentration in mixed crystals, or fully concentrated in neat compounds. Thereby, depending upon the relative energies of the excited states of the chromophores, energy-transfer is observed either from the guest system with the tris-bipyridine cations as donors to the host system where the oxalate-backbone acts as acceptor sites or *vice versa*. In addition, energy-transfer between identical chromophores occurs within the host as well as within the guest system [36, 58]. Figure 10 illustrates these energy-transfer processes schematically with different host/guest stoichiometries.

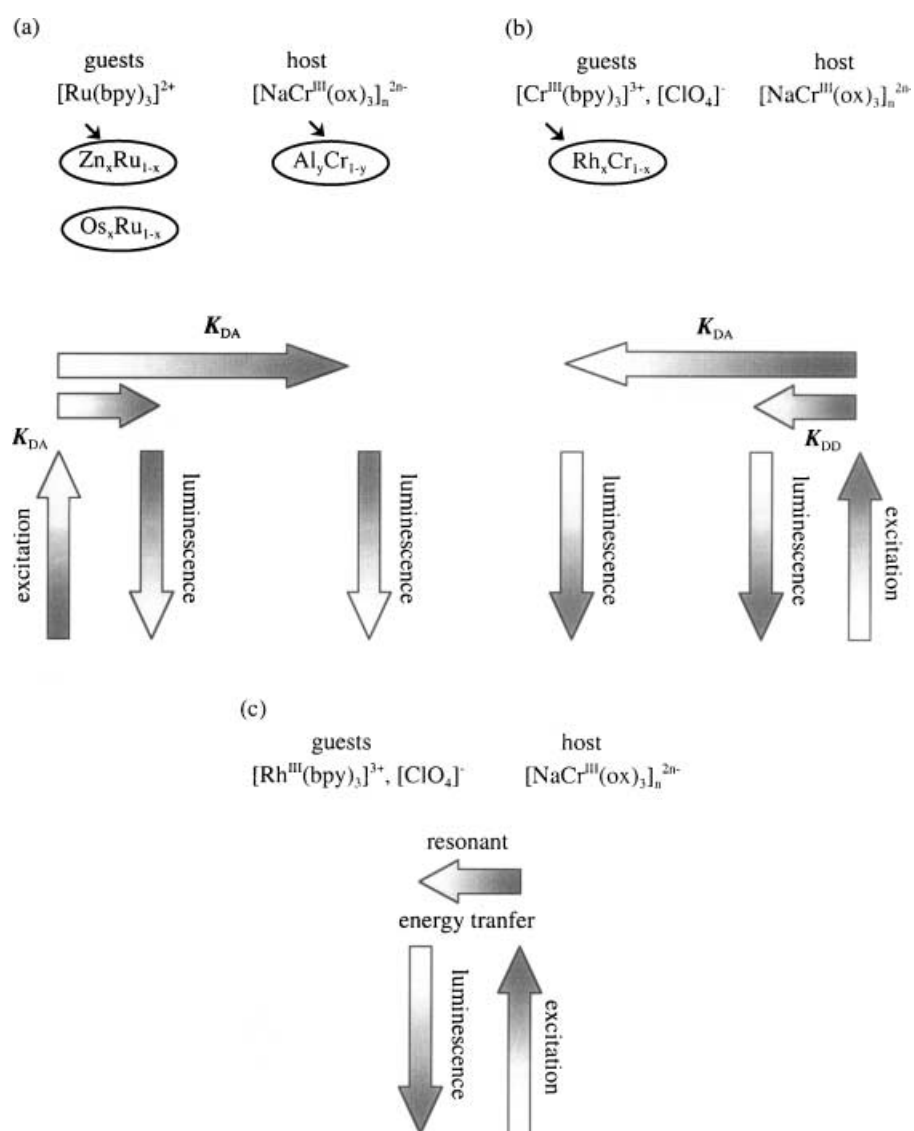


Fig. 10. Schematic representation of energy-transfer processes for different stoichiometries; excitation into the guest system (a); excitation into the host system (b) and (c)

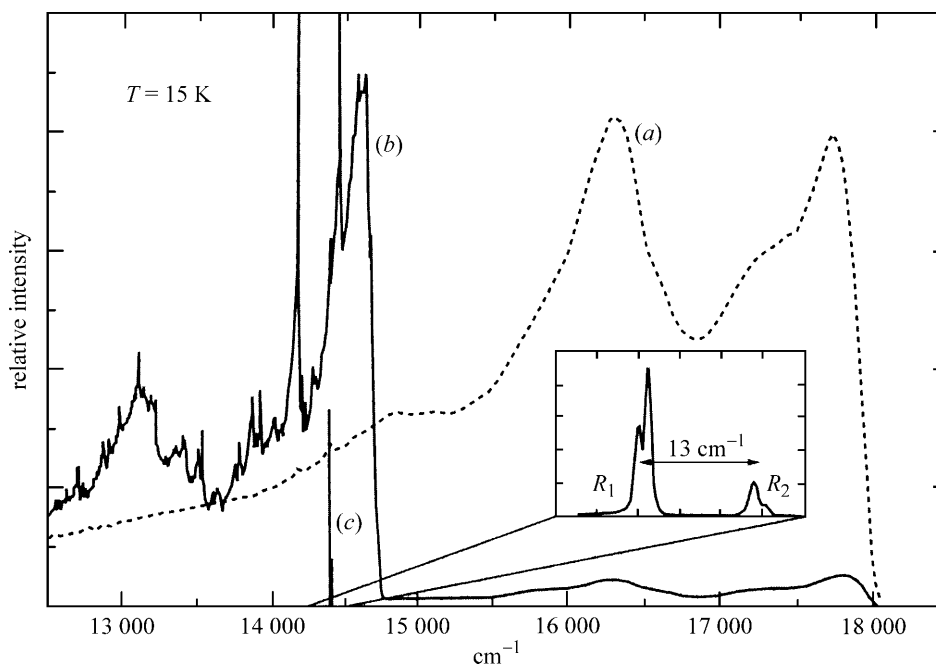


Fig. 11. Luminescence spectra at $T=15$ K of $\{[\text{Ru}(\text{bpy})_3][\text{NaAl}(\text{ox})_3]\}_n$ (a), $\{[\text{Ru}_{1-x}\text{Os}_x(\text{bpy})_3][\text{NaAl}(\text{ox})_3]\}_n$, $x=1\%$ (b), $\{[\text{Ru}(\text{bpy})_3][\text{NaCr}(\text{ox})_3]\}_n$ (c) ($\lambda=476$ nm)

As an example of the energy-transfer processes, Fig. 11 shows the luminescence spectra of three representative compounds. For instance, if Al^{3+} is replaced by Cr^{3+} , the $[\text{Ru}(\text{bpy})_3]^{2+}$ luminescence from the spin-forbidden MLCT transition is completely quenched, and the sharp luminescence bands characteristic for the zero-field components of the ${}^2\text{E} \rightarrow {}^4\text{A}_2$ transition of octahedrally coordinated and trigonally distorted Cr^{3+} are observed at 14400 cm^{-1} . This is a clear indication for very efficient energy-transfer from the initially excited $[\text{Ru}(\text{bpy})_3]^{2+}$ to $[\text{Cr}(\text{ox})_3]^{3-}$. However, not only acceptors on the oxalate-backbone may quench the $[\text{Ru}(\text{bpy})_3]^{2+}$ luminescence. Replacing a fraction of the $[\text{Ru}(\text{bpy})_3]^{2+}$ by $[\text{Os}(\text{bpy})_3]^{2+}$ results in luminescence from $[\text{Os}(\text{bpy})_3]^{2+}$ and a quenching of the $[\text{Ru}(\text{bpy})_3]^{2+}$ luminescence, too. Indeed, the energy-transfer to $[\text{Os}(\text{bpy})_3]^{2+}$ is even more efficient than to $[\text{Cr}(\text{ox})_3]^{3-}$.

Alternatively, as schematically drawn in Fig. 10(b), irradiating into the spin-allowed ${}^4\text{A}_2 \rightarrow {}^4\text{T}_2$ absorption band of $[\text{Cr}(\text{ox})_3]^{3-}$ from the host system results in intense luminescence from the ${}^2\text{E}$ state of $[\text{Cr}(\text{bpy})_3]^{3-}$ within the guest system, again demonstrating a rapid energy-transfer process. Finally, according to Fig. 10(c), the stoichiometry $\{[\text{Rh}(\text{bpy})_3][\text{ClO}_4][\text{NaCr}(\text{ox})_3]\}_n$ allows us to study the energy-transfer within the R_1 line of the ${}^2\text{E}$ state of Cr^{3+} . In that case, from a fluorescence-line-narrowing experiment, clear evidence for a resonant energy-transfer process could be gained [59, 60].

4. Concluding Remarks

Two- and three-dimensional oxalate bridged bimetallic networks appear as fruitful molecular materials to study various polyfunctional magnets with optical

properties. Their matrix organisation based on two sub-lattices permit to design a variety of hybrid materials. They offer unique opportunity to study physical fundamental properties in particular to unveil the magneto-optical relationship. Moreover, these materials may bring further developments. For instance, the fact that a specific photochromic chromophore turns out to be bistable once inserted may lead to high density optical memories if nanoparticles of the hybrid materials could be processed. Nanoparticles where all the dipolar moments of the chromophores are aligned could become electrical analogs of the so-called high spin molecules. Such examples show that properties of the whole hybrid may be considerably more than the superposition of the properties of the individual components.

References

- [1] a) *Traité des matériaux*. Presses Polytechniques Universitaires Romandes, Lausanne; b) Schubert U, Hüsing N (2000) *Synthesis of Inorganic Materials*. Wiley-VCH, Weinheim
- [2] Simon J, Bassoul P (2000) *Design of Molecular Materials*. Wiley, Chichester
- [3] a) Kahn O (1993) *Molecular Magnetism*. VCH, Weinheim; b) Lacroix PG (2001) *Chem Mat* **13**: 3495
- [4] Kurmoo M, Graham AW, Day P, Coles SJ, Hursthouse M, Caulfield JL, Singleton J, Pratt FL, Hayes W, Ducasse L, Guionneau P (1995) *J Am Chem Soc* **117**: 12209
- [5] Sato O, Iyota T, Fujijishima A, Hashimoto K (1996) *Science* **272**: 704
- [6] Ferlay S, Mallah T, Ouahes R, Veillet P, Verdager M (1995) *Nature* **378**: 701
- [7] a) Rashid S, Turner Scott S, Day P, Light ME, Hursthouse MB (2000) *Inorg Chem* **39**: 2426; b) Ohba M, Tamaki H, Matsumoto N, Okawa H (1993) *Inorg Chem* **32**: 5385; c) Alvarez S, Julve M, Verdager M (1990) *Inorg Chem* **29**: 4500; d) Cortés R, Urriaga MK, Lezama L, Arriortua MI, Rojo T (1994) *Inorg Chem* **33**: 829
- [8] Verdager M, Julve M, Michalowicz A, Khan O (1983) *Inorg Chem* **22**: 2624
- [9] a) Sunderg MR, Kikeväs R, Koskimies JK (1991) *J Chem Soc Chem Commun* **7**: 526; b) Mörtl KP, Sutter JP, Golhen S, Ouahab L, Kahn O (2000) *Inorg Chem* **39**: 1626
- [10] a) Broderick WE, Thompson JA, Godfrey MR, Sabat M, Hoffman BM (1989) *J Am Chem Soc* **111**: 7656; b) Kojima N, Aoki W, Itoi M, Ono Y, Seto M, Kobayashi Y, Maeda Yu (2001) *Solid State Commun* **120**: 165; c) Kojima N, Aoki W, Seto M, Kobayashi Y, Maeda Yu (2001) *Synth Met* **121**: 1796
- [11] a) Rochon FD, Melanson R, Andruh M (1996) *Inorg Chem* **35**: 6086; b) Andruh A, Melanson R, Stager CV, Rochon FD (1996) *Inorg Chim Acta* **309**; c) Munoz C, Julve M, Lloret F, Faus J, Andruh M (1998) *J Chem Soc Dalton Trans* 3125
- [12] a) Xu-Fang Chen, Peng Cheng, Xin Liu, Bin Zhao, Dai-Zeng Liao, Shi-Ping Yan, Zong-Hui Jiang (2001) *Inorg Chem* **40**: 2652; b) Lu JY, Lawandy A, Li Jing, Tan Yuen, Lin CL (1999) *Inorg Chem* **38**: 2695
- [13] De Munno G, Armentano D, Julve M, Lloret F, Lescouëzec R, Faus J (1999) *Inorg Chem* **38**: 2234
- [14] a) Tamaki H, Zhong ZJ, Matsumoto N, Kida S, Koikawa M, Achiwa N, Hashimoto Y, Okawa H (1992) *J Am Chem Soc* **114**: 6974; b) Tamaki H (1992) *Chem Lett* 1975
- [15] a) Decurtins S, Schmalte HW, Oswald HR, Linden A, Ensling J, Gütlich P, Hauser A (1994) *Inorg Chim Acta* **216**: 65; b) Decurtins S, Schmalte HW, Schneuwly P, Ensling J, Gütlich P, Hauser A (1994) *J Am Chem Soc* **116**: 9521
- [16] Day P (1997) *J Chem Soc Dalton Trans* 701
- [17] Coronado E, Galan-Mascaros JR, Gomez-Garcia CJ, Martinez-Agudo JM (2001) *Inorg Chem* **40**: 113

- [18] a) Ovanesyan NS, Shilov GV, Atovmyan LO, Lyubovskaya RN, Pyalling AA, Morozov YG (1995) *Mol Cryst Liq Cryst* **273**: 175; b) Ovanesyan NS, Pyalling AA, Sanina NA, Kashuba AB, Bottyan L (2000) *Hyperfine Interactions* **126**: 149
- [19] Dwyer FP, Sargeson AM (1956) *J Phys Chem* **60**: 1331
- [20] Werner A (1912) *Ber* **45**: 3061
- [21] Atovmyan LO, Shilov GV, Lyubovskaya RN, Zhilyaeva EL, Ovanesyan NS, Pirumova SI, Gusa Kovskaya IG, Morozov YG (1993) *JETP Lett* **58**: 766
- [22] Larionova J, Monbelli B, Sanchiz J, Kahn O (1998) *Inorg Chem* **37**: 679
- [23] Shilov GV, Ovanesyan NS, Sanina NA, Pyalling AA, Atovmyan LO (1998) *Russian J Coord Chem* **24**: 802
- [24] a) Carling SG, Mathonière C, Day P, Abdul Malik KM, Coles SJ, Hursthouse MB (1996) *J Chem Soc Dalton Trans* 1839; b) Mathonière C, Nutall CJ, Carling SG, Day P (1996) *Inorg Chem* **35**: 1201
- [25] a) Decurtins S, Schmalte HW, Schneuwly P, Oswald HR (1993) *Inorg Chem* **32**: 1888; b) Decurtins S, Schmalte HW, Oswald HR, Linden A, Ensling J, Gütlich P, Andreas H (1994) *Inorg Chim Acta* **216**: 65; c) Decurtins S, Schmalte HW, Pellaux R, Schneuwly P, Andreas H (1996) *Inorg Chem* **35**: 1451; d) Decurtins S, Schmalte HW, Pellaux R, Huber R, Fischer P, Ouladiff B (1996) *Adv Mater* **8**: 647; e) Pellaux R, Decurtins S, Schmalte HW (1999) *Acta Cryst* 1075
- [26] a) Hernandez-Molina, Lloret F, Ruiz-Perez C, Julve M (1998) *Inorg Chem* **37**: 4131; b) Coronado E, Galan-Mascaros JR, Gomez-Garcia CJ, Martinez-Agudo JM (2001) *Inorg Chem* **40**: 113
- [27] a) Gruselle M, Andrés R, Malézieux B, Brissard M, Train C, Verdaguer M (2001) *Chirality* **13**: 712; b) Andrés R, Brissard M, Gruselle M, Train C, Vaissermann J, Malézieux B, Jamet JP, Verdaguer M (2001) *Inorg Chem* **40**: 4633; c) Brissard M, Gruselle M, Malézieux B, Thouvenot R, Guyard-Duhayon C, Convert O (2001) *Eur J Inorg Chem* 1745; d) Brissard M, Amouri H, Gruselle M, Thouvenot R (2002) *CR Chimie* **5**: 53
- [28] Malézieux B, Andrés R, Brissard M, Gruselle M, Train C, Herson P, Troitskaya L, Sokolov V, Ovseenko S, Demeschik T, Ovanesyan N, Mamed'yarova I (2001) *J Organomet Chem* **637–639**: 182
- [29] Bénard S (2000) Thèse de l'Université de Paris XI Orsay, France
- [30] Coronado E, Galan-Mascaros JR, Gomez-Garcia CJ, Martinez-Agudo JM (1999) *Adv Mater* **11**: 558
- [31] Pei Y, Journaux Y, Kahn O (1989) *Inorg Chem* **28**: 100
- [32] Pellaux R, Schmalte HW, Huber R, Fischer P, Hauss T, Ouladiff B, Decurtins S (1997) *Inorg Chem* **36**: 2301
- [33] Iijima S, Koner S, Mizutani F (1999) *J Radioanalytical Nuclear Chem* **239**: 245
- [34] Kosterlitz DM, Thouless JM (1973) *J Phys Chem* **6**: 1181
- [35] Bhattacharjee A, Ijima S, Mizutani F (1996) *J Mag Mag Mat* **153**: 235
- [36] Decurtins S, Schmalte HW, Pellaux R, Schneuwly P, Hauser A (1996) *Inorg Chem* **35**: 1451
- [37] Andrés R, Gruselle M, Malézieux B, Verdaguer M, Vaissermann J (1999) *Inorg Chem* **38**: 4637
- [38] Sieber R, Decurtins S, Stoeckli-Evans H, Wilson C, Yufit D, Howard JAK, Capelli SC, Hauser A (2000) *Chem Eur J* **6**: 361
- [39] Coronado E, Galan-Mascaros JR, Gomez-Garcia CJ, Laukhin V (2000) *Nature* **408**: 447
- [40] Barron LD (1994) *Science* **266**: 1491
- [41] a) Rikken GLJA, Raupach E (1997) *Nature* **390**: 493; b) Rikken GLJA, Raupach E (2000) *Nature* **405**: 932; c) Raupach E, Rikken GLJA, Train C, Malézieux B (2000) *Chem Phys* **261**: 373
- [42] Caneschi A, Gatteschi D, Rey P, Sessoli R (1991) *Inorg Chem* **30**: 3936
- [43] Kumaiga H, Inoue K (1999) *Angew Chem Inter Ed Engl* **38**: 1601
- [44] Hernandez-Molina M, Lloret F, Ruiz-Perez C, Julve M (1998) *Inorg Chem* **37**: 4131

- [45] Minguet M, Luneau D, Lhotel E, Villar V, Paulsen C, Amabilino DB, Veciana J (2002) *Angew Chem Int Ed* **41**: 586
- [46] Ovanesyan NS, Shilov GV, Sanina NA, Train C, Gredin P, Gruselle M (2002) The 1th Russian Conference on High-Spin Molecule and Molecular Ferromagnets (Chernogolovka)
- [47] Troitskaya LL, Demeshchik TV, Sokolov VI, Mamed'yarova IA, Malézieux B, Gruselle M (2001) *Russian Chem Bull Intern Ed* **50**: 497
- [48] Barron LD, Buckingham AD (2001) *Acc Chem Res* **34**: 781
- [49] a) Zyss J (1994) *Molecular Non Linear Optics*. Academic Press, New York; b) Lacroix PG, Clément R, Nakatani K, Zyss J, Ledoux I (1994) *Science* **263**: 658
- [50] Bénard S, Yu Pei, Coradin T, Rivière Z, Nakatani K, Clément R (1997) *Adv Mat* **9**: 981
- [51] Bénard S, Yu P, Audière JP, Clément R, Guilhem J, Tchertaniv L, Nakatani K (2000) *J Amer Chem Soc* **12**: 9444
- [52] Evans JSO, Bénard S, Pei Y, Clément R (2001) *Chem Mater* **13**: 3813
- [53] Lacroix PG, Malfant I, Bénard S, Yu P, Rivière E, Nakatani K (2001) *Chem Mater* **13**: 441
- [54] Bénard S, Yu P (2000) *Adv Mater* **12**: 48
- [55] Bénard S, Rivière E, Yu P, Nakatani K, Delouis JF (2001) *Chem Mater* **13**: 159
- [56] a) Crano JC, Guglielmetti RJ (1999) *Organic Photochromic and Thermochromic Compounds*. Plenum Press, New York; b) (2000) *Chem Rev* **100**(5) Special Issue
- [57] Nakatani K, Yu P (2001) *Adv Mater* **13**: 1411
- [58] Von Arx M, Burattini E, Hauser A, Van Pieterse L, Pellaux R, Decurtins S (2000) *J Phys Chem A* **104**: 883
- [59] Hauser A, Riesen H, Pellaux R, Decurtins S (1996) *Chem Phys Letters* **261**: 313
- [60] Von Arx M, Hauser A, Riesen H, Pellaux R, Decurtins S (1996) *Phys Rev B* **54**: 15800